Validation of a closing procedure for fourth-order RANS turbulence models with DNS data in an incompressible zero-pressure-gradient turbulent boundary layer

S. V. Poroseva[a,*], B. E. Kaiser[a], J. A. Sillero[b], S. M. Murman[c]

[a]*Mechanical Engineering Department, University of New Mexico, Albuquerque, NM, 87131, U.S.A.*
[b]*School of Aeronautics, Universidad Politécnica de Madrid, 28040, Madrid, Spain*
[c]*NASA Ames Research Center, CA 94035, U.S.A.*

Abstract

Among factors affecting the accuracy of flow simulations with Reynolds-Averaged Navier-Stokes turbulence models is modeling turbulent diffusion processes. With the use of the Gram-Charlier series expansions, the turbulent diffusion in fourth-order one-point statistical closures of the Reynolds-Averaged Navier-Stokes equations can be modeled without introducing unknown model coefficients and without assuming turbulence being Gaussian. Terms representing turbulent diffusion processes in transport equations for second- and third-order velocity correlations do not require any modeling in such closures. In this regard, fourth-order closures are a more accurate alternative to lower-order closures where turbulent diffusion is modeled on semi-empirical or Gaussian turbulence assumptions. In the current paper, the accuracy of the closing procedure based on the Gram-Charlier series expansions is evaluated using data of direct numerical simulations in an incompressible zero-pressure-gradient turbulent boundary layer over a flat plate. One-point third-, fourth-, and fifth-order velocity moments were extracted for this purpose from the dataset collected by the Fluid Dynamics Group at the Universidad Politécnica de Madrid at two streamwise locations $Re_\theta = 4101$ and 5200 that correspond to channels and pipes at $\delta^+ = 1331$ and 1626. Results demonstrate that the truncated Gram-Charlier series

* Corresponding author. E-mail address: poroseva@unm.edu

expansions are an accurate approximation of the fifth-order velocity moments in the considered flow.

Keywords: DNS, boundary layer, high-order statistics, Gram-Charlier series expansions

1. Introduction

The Reynolds-Averaged Navier-Stokes (RANS) approach to turbulence modeling has the potential for producing turbulent flow solutions that are infinitely close to the solution of the Navier-Stokes equations. The solution of the complete set of RANS equations consists of velocity moments of different orders: $\overline{u_i^n u_j^m u_k^l}$, where u_i is a velocity fluctuation in the *i*-direction, $n + m + l \geq 2$, where $n,\ m,\ l = 0, 1, \dots, \infty$, and "—" over a parameter indicates the statistical mean value of the parameter. Being statistical moments, velocity correlations completely describe the turbulent flow field similar to the probability density function (Chou, 1945).

In the general case, an infinite number of correlations $\overline{u_i^n u_j^m u_k^l}$ is required to completely describe a turbulent flow field. In practice, only some flow characteristics and their accurate representation are of importance. Therefore, only those velocity moments that are linked to the flow characteristics of interest need to be reproduced accurately. This leads to the "closure" procedure, in which the complete set of RANS equations is closed, in a sense that only transport equations for velocity moments of a specified order ($s = n + m + l$) and below are solved. Velocity moments of higher orders ($n + m + l > s$) are modeled in terms of a chosen set of lower-order turbulence statistics. The highest order of velocity moments for which transport equations are solved provides a basis for categorizing a closure as first order ($s = 1$), second order ($s = 2$), etc. Thus, in the absence of modeling assumptions, the family of RANS closures

can be viewed as a hierarchy, with increasing closure order providing an increasingly accurate representation of the complete set of RANS equations.

While closure models up to the fourth order were proposed as far back as the 1940's (Monin and Yaglom, 1979), most engineering predictions today use first-order closure models (one- and two-equation RANS models), where all turbulence effects are modeled based on empirical/intuitive considerations. Such models are known for not consistently predicting many engineering flows of interest, especially those with separation (Johansson and Davidson, 2006; Leschziner, 2006; Rumsey et al., 2004; Thiele and Jakirlic, 2007; Vassberg et al., 2014). In second-order RANS closures (Reynolds stress transport models), third-order velocity moments are usually modeled using a semi-empirical generalized gradient-diffusion hypothesis (Chou, 1945; Daly and Harlow, 1970). Models based on this hypothesis, or of similar kind (see, for example, Hanjalić and Launder, 2011; Younis et al. 2000; Nagano and Tagawa, 1988) include unknown coefficients and tend to fail when compared with experimental data (Hanjalić and Launder, 2011; Kurbatskii and Poroseva, 1999; Nagano and Tagawa, 1988; Parneix et al., 1998; Schwarz and Bradshaw, 1994).

In third-order RANS closures, the fourth-order velocity moments modeling can be directly linked to the statistical properties of a turbulent flow field, for example, using Millionshtchikov's hypothesis of quasinormality (Millionshtchikov, 1941),

$$\overline{u_i u_j u_k u_l} = \overline{u_i u_j} \cdot \overline{u_k u_l} + \overline{u_i u_k} \cdot \overline{u_j u_l} + \overline{u_i u_l} \cdot \overline{u_j u_k}. \quad (1)$$

The quasinormality hypothesis is based on the assumption of the Gaussian distribution of the probability density function (PDF) of the turbulent velocity field for fourth- and higher-order

order velocity moments, and does not introduce any unknown model coefficients. In this regard, third-order closures based on (1) are an improvement to compare with lower-order closures. The validity of Millionshtchikov's hypothesis was demonstrated for one-point statistics in a few experiments starting from Uberoi (1953) and for two-point statistics in Zaets et al. (1984). However, a turbulent velocity field is generally non-Gaussian (for detailed discussion, see Ch.6 in Tsinober, 2001) that limits the applicability area of (1) as a model.

Various possibilities of representing the PDF of a non-Gaussian turbulent velocity field in terms of the degree of its deviation from a Gaussian form were analyzed in Kampé de Fériet (1966). As a result, the Gram-Charlier series expansions were proposed for this purpose. In such expansions, a non-Gaussian PDF is given in the form of a series in Hermite polynomials for two variables with respect to the Gaussian distribution. The two-dimensional form of such a PDF can be found in Frenkiel and Klebanoff (1973) and Durst et al. (1993), for example.

By truncating the Gram-Charlier series expansions to the fourth and higher orders, one can express higher-order velocity moments in terms of lower-order ones. The following expressions for the fifth-order velocity moments:

$$\overline{u_i^5} = 10\overline{u_i^2}\cdot\overline{u_i^3}\,,$$

$$\overline{u_i^4 u_j} = 6\overline{u_i^2}\cdot\overline{u_i^2 u_j} + 4\overline{u_i^3}\cdot\overline{u_i u_j}\,, \tag{2}$$

$$\overline{u_i^2 u_j^3} = 6\overline{u_i u_j}\cdot\overline{u_i u_j^2} + \overline{u_i^2}\cdot\overline{u_j^3} + 3\overline{u_i^2 u_j}\cdot\overline{u_j^2}\,.$$

were obtained by truncating the Gram-Charlier series expansions to the fourth order. Expressions (2) and similar ones for higher-order correlations do not contain unknown coefficients and can be used for closing a set of RANS equations. The lowest RANS closure order for which this procedure can be applied is the fourth order. Notice that in Frenkiel and Klebanoff (1973), concerns were brought to attention that truncating the Gram-Charlier series expansions may lead to negative values in the PDF in some cases. Experiments conducted by Antonia and Atkinson (1973) and Nakagawa and Nezu (1977) did not reveal such a problem. Even if such cases exist, the only way to identify them is to continue empirically testing the truncated Gram-Charlier series expansions in various flows. To date, the applicability of Gram-Charlier series expansions has been successfully tested against experimental data in the turbulent boundary layer on a flat plate (Antonia and Atkinson,1973; Durst et al., 1993; Frenkiel and Klebanoff, 1973), and an open-channel flow over smooth and rough surfaces (Nakagawa and Nezu, 1977). Good agreement between experimental data (Bukreev et al., 1975; Pilipchuk, 1986) and the predictions using the Gram-Charlier series expansions was also observed in a cylindrical pipe flow (Kurbatskii and Poroseva, 1997; Poroseva, 1996).

With existing experimental techniques, only a few high-order velocity moments can accurately be measured. A further progress in validating the truncated Gram-Charlier series expansions as a closing procedure can be achieved with direct numerical simulations (DNS) of the Navier-Stokes equations that have fully matured as a research tool (Moin and Mahesh, 1988) capable of providing experimental-quality data. Recently, DNS data were used for validating expressions (2) in a two-dimensional (2D) channel (Jeyapaul et al., 2014) at $Re_\tau = 392$, where Re_τ is based on the friction velocity u_τ and the channel half-height. The goal of the current paper

is to validate expressions (2) with DNS data in a two-dimensional zero-pressure-gradient (ZPG) turbulent boundary layer over a flat plate.

Notice that prior modeling dissipation processes and velocity/pressure-gradient correlations in transport equations through the fourth order in planar flows, only models for fifth-order velocity moments for two variables – $\overline{u^5}$, $\overline{u^4v}$, $\overline{u^3v^2}$, $\overline{u^2v^3}$, $\overline{uv^4}$, $\overline{v^5}$ – are required to close the set of equations. Thus, expressions (2) will be sufficient to serve the purpose, and this is why they are of interest for the current study. However, moments $\overline{u^2vw^2}$ and $\overline{uv^2w^2}$ are also present in planar flows and may be required for modeling purposes. Fifth-order moments for three variables will be necessary in three-dimensional flows as well. To the best of our knowledge, the model representation for such moments has yet to be developed. Therefore, they are not considered in the paper.

The DNS data for higher-order velocity moments were extracted from the raw DNS dataset collected by the Fluid Dynamics Group at the Universidad Politécnica de Madrid at two streamwise locations Re_θ = 4101 and 5200 (Borrell et al., 2013; Sillero et al., 2013; Simens et al., 2009), where Re_θ is based on the free stream velocity and the boundary layer momentum thickness θ. Second-order pressure-velocity central moments are also provided. Such data are usually not available (Tsuji et al., 2007), but necessary for better understanding and modeling the interaction of turbulent velocity and pressure fields.

2. DNS data

The DNS database reported in the current paper is collected at relatively high Reynolds numbers: Re_θ = 4101 and 5200 at which some experimental data are available (DeGraaff and Eaton, 2000; Schwarz, 1992). Experimental (Klewicki, 1989; Smith, 1994) and DNS (Schlatter

and Örlü, 2010) data at Reynolds numbers: Re_θ = 4980, 4850, and 4060 are also used for comparison.

Direct numerical simulations of a ZPG turbulent flow over a flat plate were conducted with periodic spanwise boundary conditions and non-periodic streamwise and wall-normal boundary conditions. A precursor low-resolution simulation was used to minimize the flow development distance and the outflowing turbulent field of the precursor simulation was passed to the main high-resolution simulation, hereafter, $BL_{6600,}$ by rescaling the turbulent field. The primitive-variable formulation of the incompressible Navier-Stokes equations was solved using a fractional-step method to ensure mass conservation. Spatial derivatives in the streamwise and wall-normal directions were computed using staggered three-point compact finite differences with the exception of the Poisson equation for pressure, which was computed with second-order finite differences (with no penalty in the global accuracy of the code). A Fourier spectral representation was used for the variables in the spanwise direction, dealiased using the 2/3 rule. Time was advanced using a semi-implicit, three-step Runge-Kutta scheme. A detailed description of the simulation procedure and the first- and second-order one-point statistics can be found in Borrell et al. (2013), Sillero et al. (2013), and Simens et al. (2009).

In Sillero et al. (2013), the domain of BL_{6600} extends from $Re_\theta = 2780$ to 6680 in the streamwise direction, and the ratio of the domain height to the boundary layer thickness at the exit plane is approximately 2.5. Here, higher-order turbulence statistics collected at $Re_\theta = 4101$ and 5200 are reported. At $Re_\theta = 5200$, all relevant flow scales are correctly represented (Sillero et al., 2013). Simulation and comparison with experiment data was deemed permissible at $Re_\theta = 4101$, because the maximum Reynolds stress, δ/θ (where δ is the boundary layer thickness), and the wake intensity are close to convergence at $Re_\theta = 4101$ (Sillero et al., 2013),

and the second-order statistics collected by the Hot Wire Anemometry (HWA) experiment are up to 15% uncertainty (Schwarz, 1992).

To obtain turbulence statistics, DNS data were averaged in the spanwise direction over 4096 cells for both Reynolds numbers and over different time realizations: 207 and 209 for $Re_\theta = 4101$ and 5200, respectively. Total non-dimensional time over which the statistics are compiled is 11.5 turnovers ($= t \cdot u_\tau/\delta$) in the middle of computational box, which corresponds to $Re_\theta = 4850$ (Sillero et al., 2013). Local times are 13.6 and 10.6 for $Re_\theta = 4160$ and 5200, respectively. The spanwise direction was assumed to be statistically homogeneous, and data collected at different times were assumed uncorrelated (Sillero et al., 2013). To increase a number of samples used for averaging, data collected in a short region in the streamwise direction, where the boundary layer thickness growth did not exceed 1.22%, was also used. It gave additional 198 and 247 realizations at $Re_\theta = 4101$ and 5200, respectively. The analysis of aliasing errors in averaged data showed them to be marginal.

In Figure 1, DNS profiles of the third-order velocity moments are shown. Hereafter, velocity fluctuations *u, v,* and *w* are in the streamwise, normal-to-the-wall, and spanwise flow directions, respectively. The "+" notation signifies normalization by the friction velocity u_τ, and $y_+ = yu_\tau/\nu$, where ν is the kinematic viscosity. The skewness and flatness factors are given in Fig. 2. Figure 3 demonstrates fourth- and fifth-order velocity moments for velocity fluctuations in the streamwise and wall-normal directions. Additional fifth-order velocity moments are provided in the following section. Figure 4 shows the pressure-velocity moments. The database of all generated moments can be downloaded from the website of the first author.

A slight variation in the DNS profiles obtained at $Re_\theta = 4101$ and 5200 is observed, but this difference is expected (Alfredsson, 2011; DeGraaff and Eaton, 2000; DeGraaff et al., 1998;

Honkan and Andreopoulos, 1997; Murlis et al., 1982; Österlund, 1999). An agreement between the DNS profiles and available experimental data at close Reynolds numbers is good for all moments, except those with velocity fluctuations in the wall-normal direction. Such moments are known to be more challenging to measure (Alfredsson, 1988; DeGraaff and Eaton, 2000; Hutchins et al., 2009; Ligrani and Bradshaw, 1987; Nagano and Tsuji, 1994; Smits et al., 2011), and thus, the agreement is only qualitative. The agreement for the skewness factor S_v is better (Fig. 2a), than for $\overline{v^3}^+$ (Fig. 1d), that is, when uncertainties associated with measuring the friction velocity are eliminated from comparison.

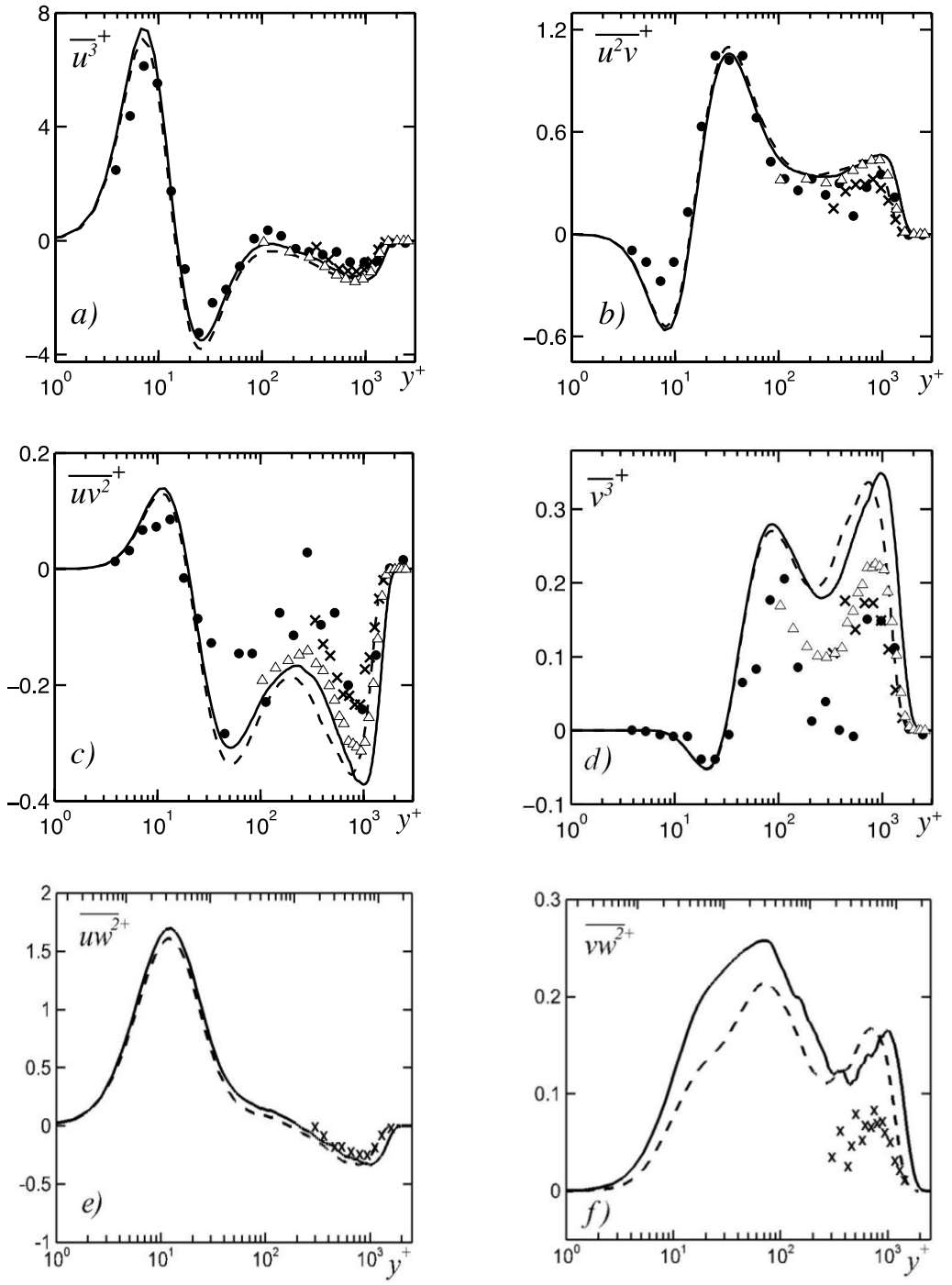

FIG. 1. Third-order velocity moments. Notations: - - - BL_{6600} at $Re_\theta = 4101$, ——— BL_{6600} at $Re_\theta = 5200$, × Schwarz (1992) at $Re_\theta = 4101$, ● DeGraaff and Eaton (2000) at $Re_\theta = 5200$, △Smith (1994) at $Re_\theta = 4980$.

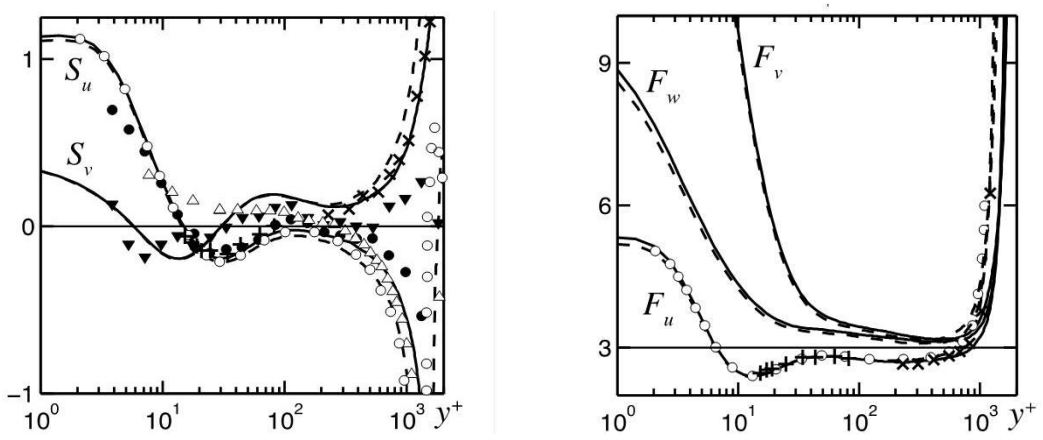

a) *b)*

FIG. 2. Skewness and flatness factors. Notations: - - - BL_{6600} at $Re_\theta = 4101$, ——— BL_{6600} at $Re_\theta = 5200$, × Schwarz (1992) at $Re_\theta = 4101$, ●, ▼ DeGraaff and Eaton (2000) streamwise and wall-normal skewness, respectively, at $Re_\theta = 5200$, ▵Smith (1994) streamwise skewness at $Re_\theta = 4980$, ○ Schlatter and Örlü (2010) streamwise parameters at $Re_\theta = 4060$, + Klewicki (1989) streamwise parameters at $Re_\theta = 4850$.

To quantify the DNS data uncertainty, standard deviations of relevant velocity fluctuations products $u_i^n u_j^m u_k^l$ were collected. The standard deviation of a given product was first evaluated for each time realization using the product data in the spanwise direction at each *y*-location:

$$\sigma_z(y)\big|_{t=t_j} = \sqrt{\frac{1}{N_z}\sum_{i=1}^{N_z}\left(f_i(y) - \overline{f}(y)\right)^2}\,, \tag{3}$$

where $f(y)$ is the velocity fluctuations product, $u_i^n u_j^m u_k^l$, with the specified *n*, *m*, and *l*; $\overline{f}(y)$ is its mean, velocity moment $\overline{u_i^n u_j^m u_k^l}$; N_z is the sample size in the streamwise direction equal to 4096 for both Reynolds numbers; and t_j is a time realization. The estimate of $\sigma_z(y)$ was improved by averaging its values over different time realizations and different locations in the streamwise direction:

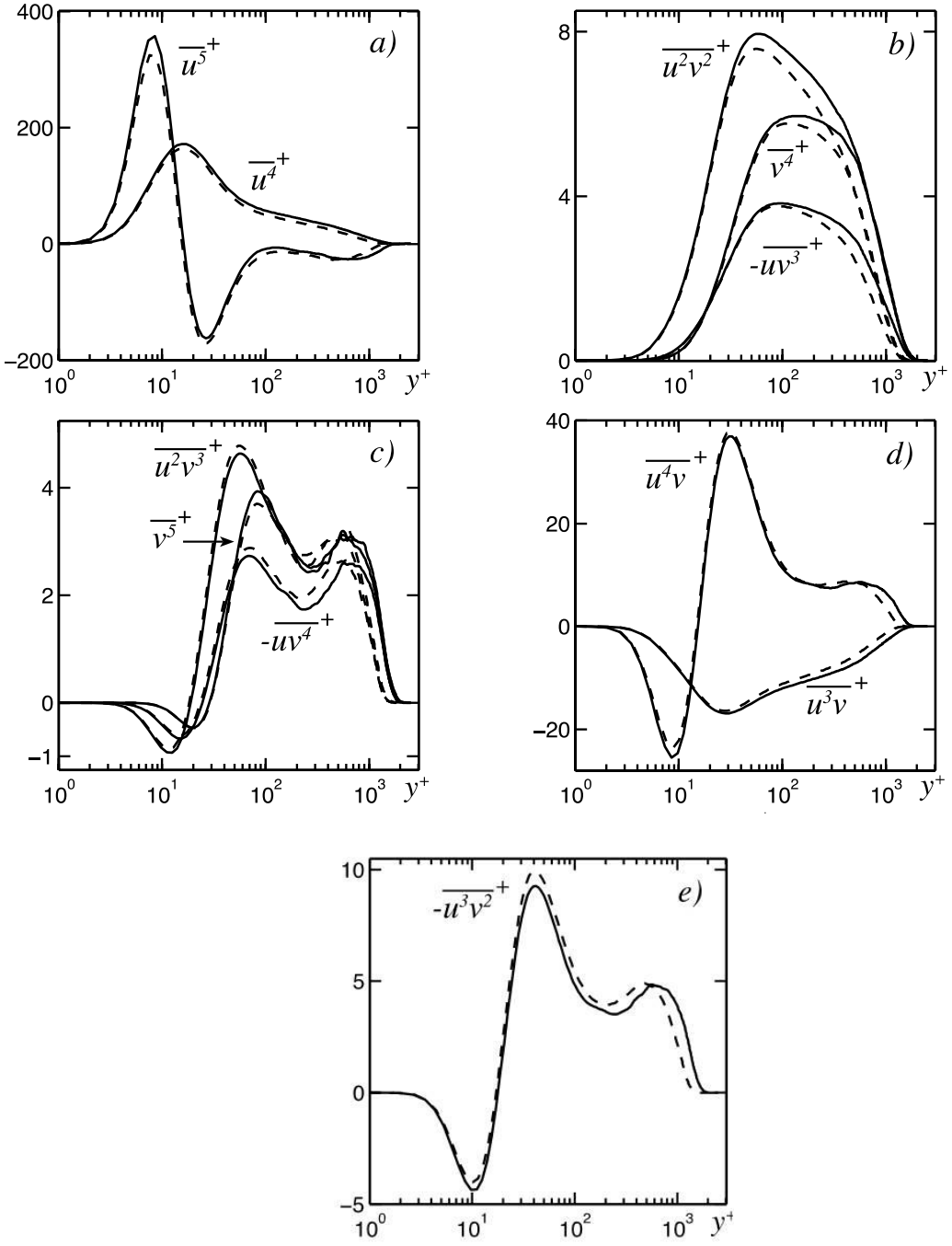

FIG. 3. Fourth and fifth-order velocity moments for velocity fluctuations in the streamwise and wall-normal directions. Notations: - - - BL_{6600} at $Re_\theta = 4101$, ——— BL_{6600} at $Re_\theta = 5200$.

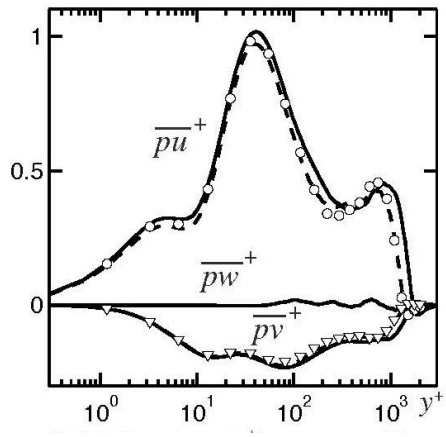

FIG. 4. Pressure-velocity moments, BL_{6600} at $Re_\theta = 4101$ and 5200. Symbols represent Schlatter and Örlü (2010) at $Re_\theta = 4060$.

$$\sigma_t(y)\big|_{x=x_k} = \sqrt{\frac{1}{N_t}\sum_{j=1}^{N_t}\sigma_z^2(y,t_j)} \quad \text{and} \quad \sigma(y) = \sqrt{\frac{1}{N_x}\sum_{k=1}^{N_x}\sigma_t^2(y,x_k)}\,, \tag{4}$$

where (N_t, N_x) are (207,198) and (209,247) for $Re_\theta = 4101$ and 5200, respectively.

The standard deviation of the velocity fluctuations product mean (the mean of a velocity moment) can be obtained from $\sigma_z(y)$ as $\sigma_{\bar{f}}(y) = \sigma_z(y)/\sqrt{N_z}$ assuming the normal mean distribution. (Here, we used the improved estimate for $\sigma_z(y)$, $\sigma(y)$.) The assumption is valid for a sample size larger than 30 (Theorem 8.2 in Walpole, 1969). With N_z= 4096, the assumption is satisfied.

Figure 5 shows absolute values of the coefficient of variation $CV = \sigma_{\bar{f}}/\bar{f}$ for velocity moments $\bar{f} = \overline{u_i^n}$, where *n* = 2, 3, 4, and 5. Coefficients of variation of the even-order moments are given in Fig. 5a and for odd-order moments in Fig. 5b for $Re_\theta = 5200$. The coefficient of variation is known to be not a reliable metric when the mean is very close to zero. This is why the profiles are shown in the range of $10 < y_+ < 1500$ (omitting the areas next to the wall and

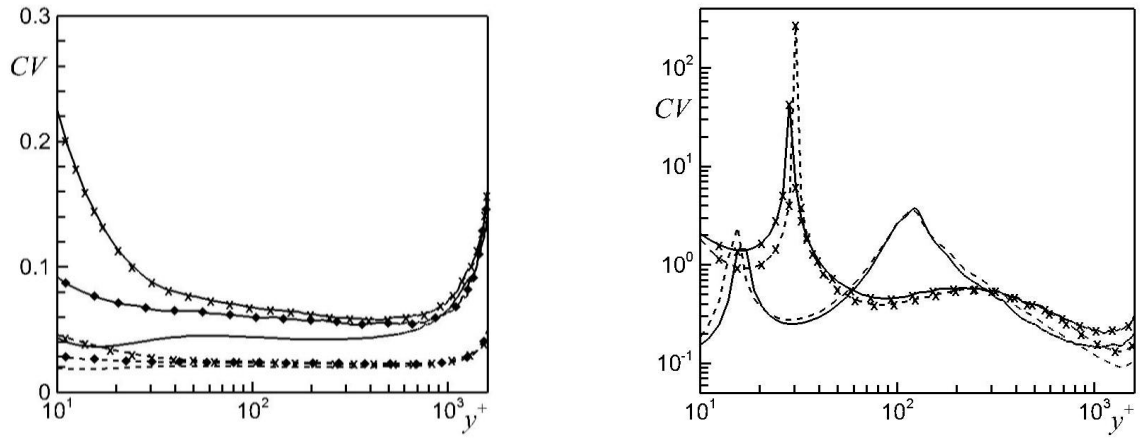

a) *b)*

FIG. 5. The coefficient of variation for *a)* even-order velocity moments and *b)* odd-order moments at $Re_\theta = 5200$. Notations: ----- $\overline{u^2}$, $\overline{u^3}$; —— $\overline{u^4}$, $\overline{u^5}$; --×-- $\overline{v^2}$, $\overline{v^3}$; —×— $\overline{v^4}$, $\overline{v^5}$; --♦-- $\overline{w^2}$; —♦— $\overline{w^4}$.

the boundary layer edge) in both figures. The picks observed in Fig. 5b are also due to the odd-order moments changing the sign in those areas. Figure 5a demonstrates that the coefficient of variation increases with the order of even-order moments. The effect is less noticeable for the odd moments except in the outer half of the boundary layer at $y_+ > 800$.

No significant difference is observed in the coefficients of variation of different second-order moments (Fig. 5a), but the difference appears for higher-order moments. In particular, the coefficients of variation of velocity moments in the streamwise direction tend to be lower than for the moments in spanwise and normal-to-the-wall directions.

3. Closing procedure validation

The data presented in Fig. 1 along with the second-order velocity moments (not shown here, but in agreement with those reported in Sillero et al., 2013) were used to verify expressions (2) for the fifth-order one-point correlations between any two velocity fluctuations. Results of comparing DNS profiles for the fifth-order velocity moments (solid lines) with those obtained

from expressions (2) (dashed lines) using DNS data for lower-order velocity moments are shown in Fig. 6 at Re_θ = 4101 (blue lines) and 5200 (black lines).

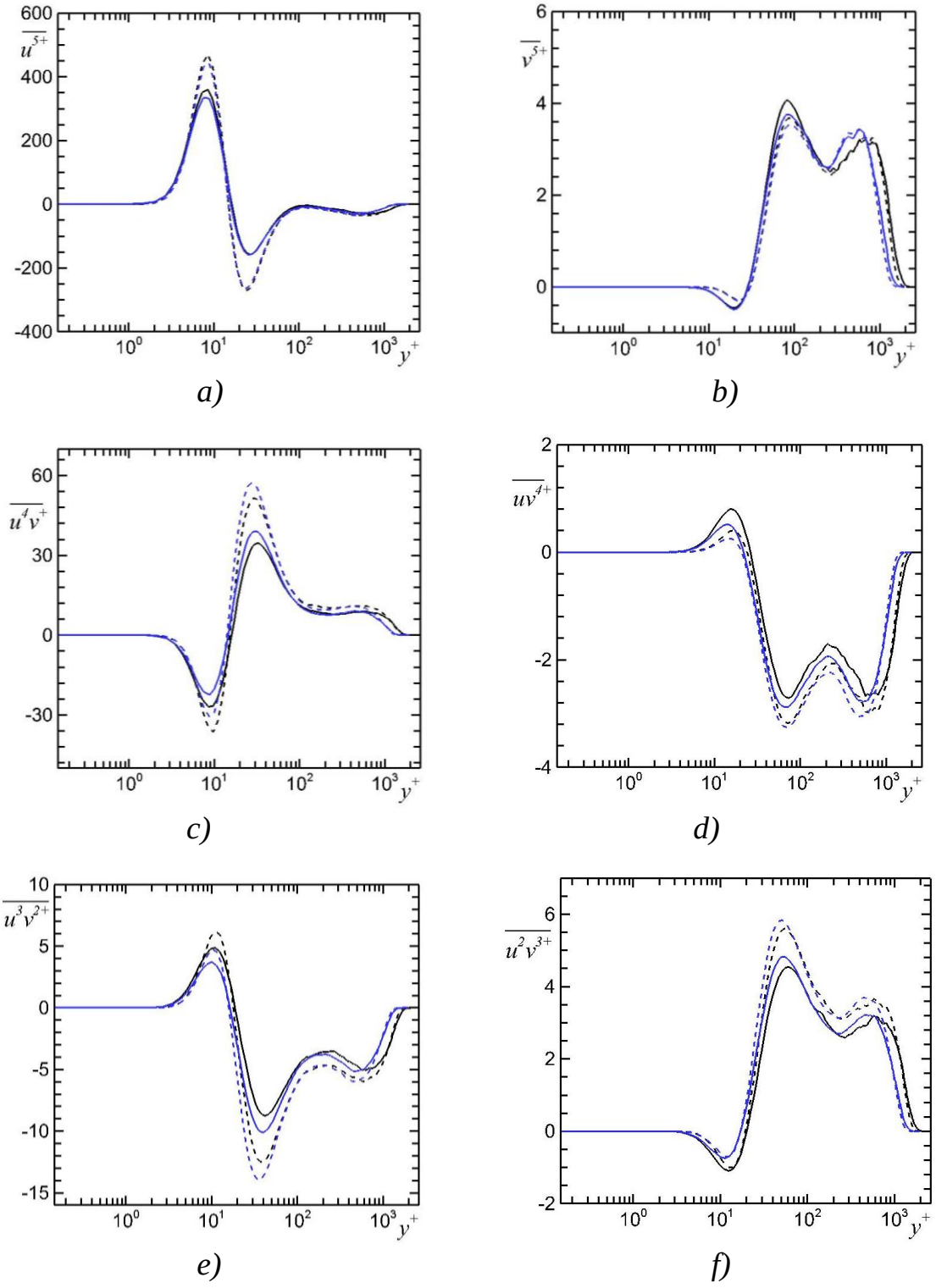

FIG. 6. (continued on the next page).

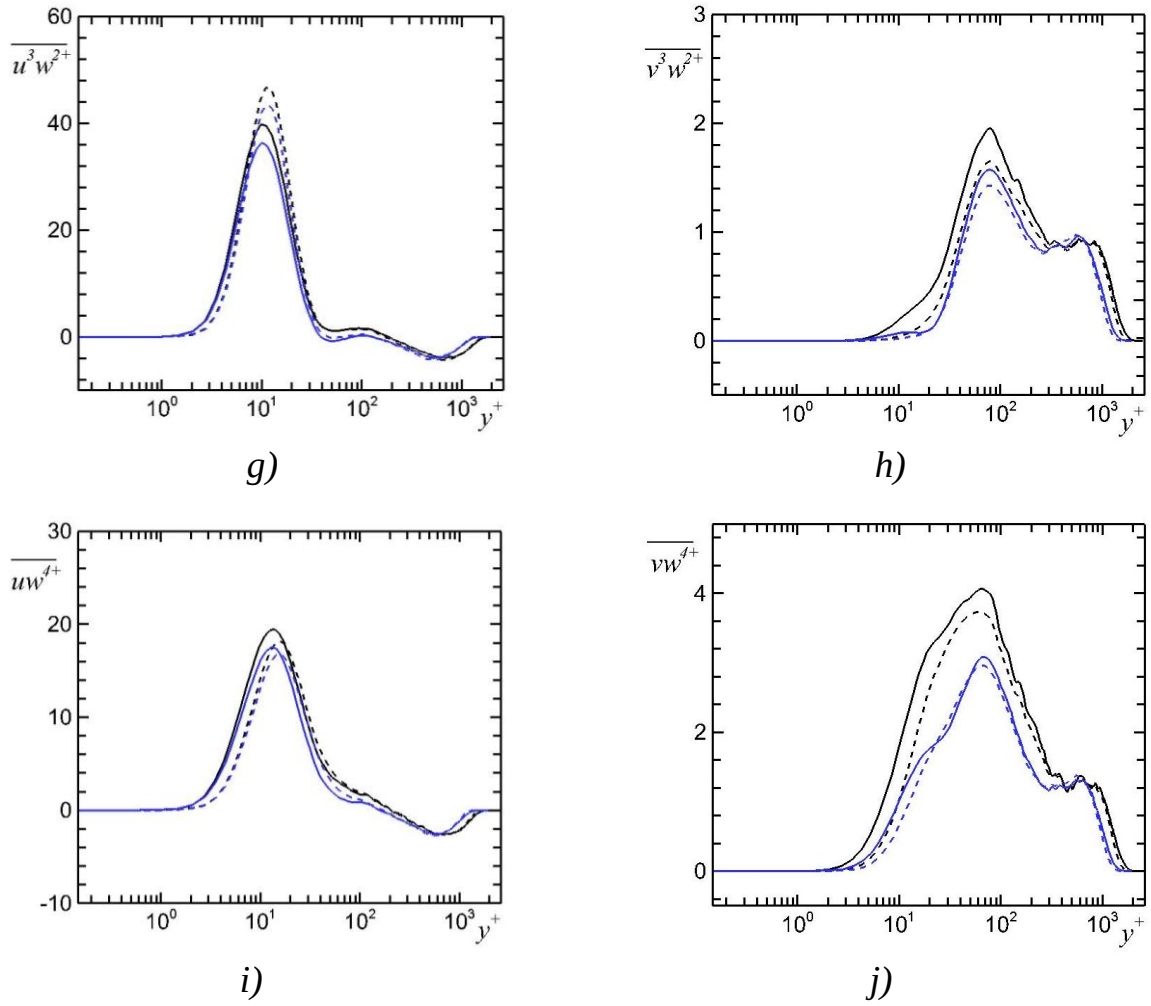

FIG. 6. Profiles of fifth-order velocity correlations in the zero-pressure gradient boundary layer over a flat plate at $Re_\theta = 4101$ (blue lines) and $Re_\theta = 5200$ (black lines). Notations: — DNS fifth-order velocity moments, - - profiles calculated from the truncated Gram-Charlier series expansions (2) using DNS data for lower-order moments. DNS data for the second-order velocity moments are from Sillero et al. (2013).

Figure 6 demonstrates that the truncated Gram-Charlier series expansions are a good approximation for all considered fifth-order moments. Some discrepancy between the fifth-order moments and their Gram-Charlier series expansions predictions is observed, but this is expected when comparing data of statistical observations. The discrepancy is higher around moments' extremes. No Reynolds number effect within the considered range was detected for this effect

either. Similar tendencies for fifth-order velocity moments and their Gram-Charlier series expansions predictions were observed in a two-dimensional fully-developed channel flow (Jeyapaul et al., 2014) at $Re_\tau = 392$.

In the areas around moments' extremes, the standard deviation values are also at maximum. As an example, the 95%-confidence intervals ($\pm 2\sigma_{\bar{f}}(y)$) for the fifth-order velocity moment in the streamwise direction (black lines) and its Gram-Charlier series expansions prediction (blue lines) are shown in Fig. 7 along with their overlapping area (between two red lines). The level of confidence was estimated assuming the normal distribution for all relevant moments (Walpole, 1969). For symmetrical unimodal distributions and for any unimodal distributions, more conservative confidence estimates can also be applied: Bienaymé-Chebyshev (Bienaymé, 1853; Chebyshev, 1867) (often just Chebyshev) and Vysochanskij-Petunin (Sellke and Sellke, 1997; Vysochanskij and Petunin, 1980, 1983) inequalities, respectively. The former inequality assigns confidence of 75% to the 2σ-interval, and the latter gives the estimate of 89%. The error propagation rules (Ku, 1966) for independent functions were used to evaluate the standard deviation of the Gram-Charlier series expansions predictions, which is accepted practice in the analysis of statistical data when no information on the functions dependence is available. As the figure demonstrates, the overlapping exists everywhere within the boundary layer. Thus, the Gram-Charlier series

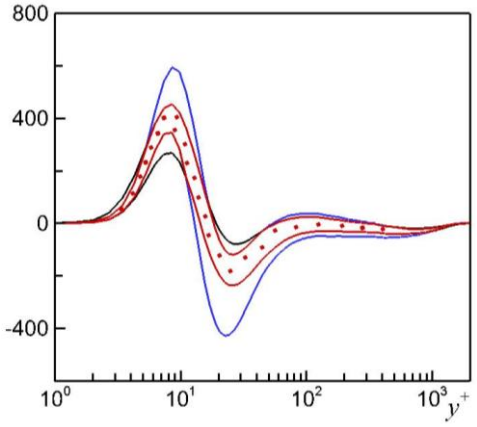

FIG. 7. The areas of 95%-confidence intervals for $\overline{u^{5+}}$ (marked by black lines), its Gram-Charlier series expansions prediction (Eq. (2)) (blue lines) and their overlap (red lines) at $Re_\theta = 5200$.

expansions do approximate the true value of the fifth-order moment with the specified level of confidence. Similar results were obtained for the other fifth-order moments (not shown here).

A statistical approach to evaluating the significance of the discrepancy between two sample means is testing the null hypothesis that the difference between the true means approximated by the sample means is equal to zero (see, for example, Ch. 10 in Walpole, 1969, for testing statistical hypothesis). If the hypothesis holds true, then a value determined as

$$z = \frac{\left(\overline{f_1} - \overline{f}_2\right)}{\sqrt{\sigma^2_{\overline{f_1}} + \sigma^2_{\overline{f_2}}}}, \tag{5}$$

is a value of the standard normal variable Z when sample sizes are large (N > 30) and the independence of f_1 and f_2 is assumed. If the hypothesis is not correct, $Z < -z_\alpha/2$ and $Z > z_\alpha/2$, where α is the level of significance and $(1-\alpha)\cdot 100\%$ is the confidence level. For $\alpha = 0.05$, the hypothesis is violated when $Z < -1.96$ and $Z > 1.96$.

When comparing the fifth-order moments with the Gram-Charlier series expansions predictions, $\overline{f_1}$ and $\overline{f_2}$ are a fifth-order moment and its prediction from expressions (2), respectively. For the 95%-confidence level, Z-profiles for all fifth-order moment from Fig. 6 are shown in Fig. 8. As the figure demonstrates, the hypothesis that the Gram-Charlier series expansions predictions approximate the same true means as the corresponding fifth-order velocity moments holds true within the boundary layer except towards the boundary layer edge. This is the area where velocity moments are close to zero (Figs. 1, 3, and 6). When comparing values close to zero, it is difficult to point the single source of the discrepancy between them.

Regardless the error source, the difference between the moments and their predictions is less significant due to their small values.

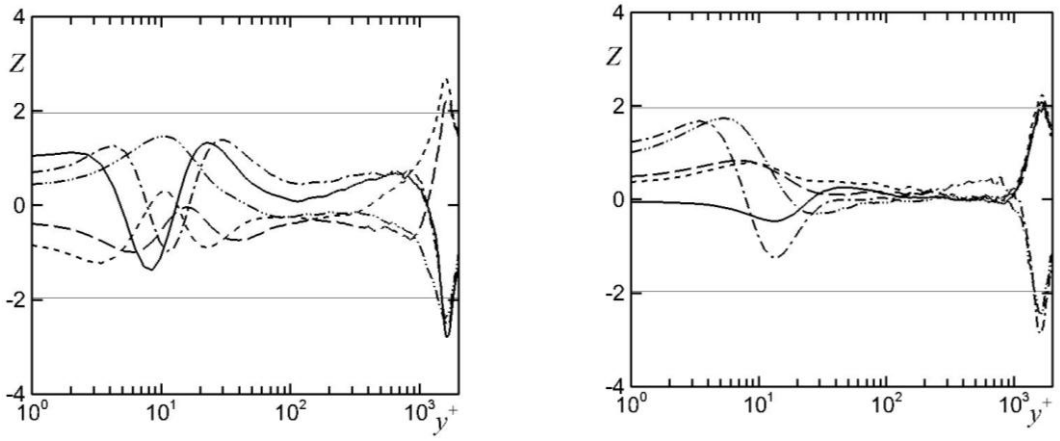

FIG. 8. The Z-profiles (Eq. (5)) for the fifth-order velocity moments. Notation: grey solid lines are at $Z = \pm 1.96$ that corresponds to the 95%-confidence interval; lines ——, - - -, $-\cdot-$, $--$, and $-\cdot\cdot-$ correspond to $\overline{u^5}$, $\overline{u^4v}$, $\overline{u^3v^2}$, $\overline{u^2v^3}$, and $\overline{uv^4}$, respectively, in Fig. 8a and to $\overline{v^5}$, $\overline{v^3w^2}$, $\overline{u^3w^2}$, $\overline{vw^4}$, and $\overline{uw^4}$ in Fig. 8b.

In addition to the statistical nature of DNS data, other factors may contribute as well in the observed discrepancy between DNS data and profiles predicted with truncated Gram-Charlier series expansions. Close to the wall, both flows may not be planar, but three- dimensional. In the boundary layer, this effect is mainly manifested for the third-order velocity moments $\overline{w^3}$ and $\overline{u^2w}$ (other second- and third-order moments that have to be zero in planar flows are negligible). As shown in Fig. 9, the magnitude of these moments is comparable with that of $\overline{v^3}$ in the buffer zone. Experimental data (Ölçmen et al., 1999; Schwarz, 1992) support this observation. In the channel flow (Jeyapaul et al., 2014), the moment $\overline{uw}$ is at maximum in the same area where the maximum discrepancy is observed between DNS and predicted profiles for the fifth-order velocity moments. The $\overline{uw}$-moment is smaller than $\overline{uv}$, but not negligible like $\overline{vw}$. The observed

three-dimensionality may be a physical property of near-wall flows, or possibly induced by inaccuracies of DNS and experimental techniques used in the wall area.

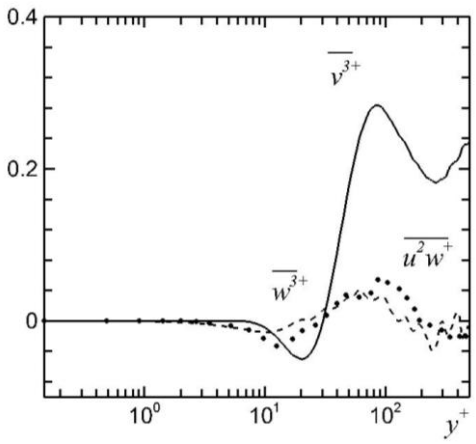

FIG. 9. The planar flow assumption validation using DNS data at $Re_\theta = 5200$ in a zero-pressure gradient boundary layer over a flat plate. Notations: — $\overline{v^{3+}}$, - - $\overline{w^{3+}}$, and ··· $\overline{u^2w^+}$.

To better illustrate the importance of using higher-order closures in wall-bounded flows, DNS profiles for the fourth-order moments are compared in Figs. 2 and 10 with those obtained from Millionshtchikov's hypothesis (1) using DNS data for second-order moments. In Figure 2, the solution for the Gaussian velocity distribution (S = 0, F = 3) are shown by horizontal lines. In Figure 10, DNS profiles for the fourth-order moments are shown by dashed lines and the profiles obtained from the quasinormality hypothesis, by solid lines. The figures demonstrate that the assumption of a Gaussian turbulent velocity field is weak in the considered flow: it is a good approximation for $\overline{uv^3}$ and $\overline{u^2v^2}$, but gives only qualitative agreement for $\overline{u^3v}$. For the flatness factors shown in Fig. 2, this hypothesis can be used as an approximation far from the wall and from the boundary layer edge. Regions of the near-Gaussian behavior of the velocity skewness and flatness factors are in agreement with those identified in Durst et al. (1993).

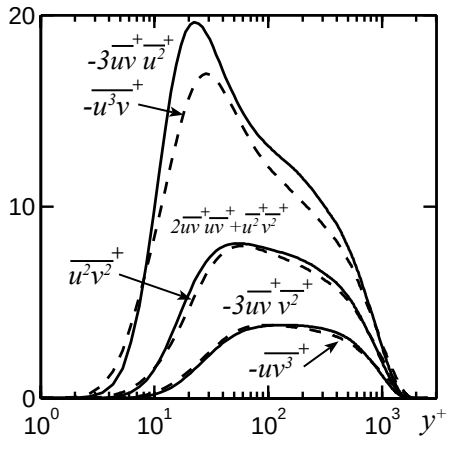

FIG. 10. Comparison of the DNS fourth-order velocity moments with the profiles obtained from the quasinormality hypothesis using DNS data for the second-order moments at $Re_\theta = 5200$.

4. Conclusion

The accuracy of the truncated Gram-Charlier series expansions in representing fifth-order velocity moments in terms of lower-order velocity moments is evaluated using DNS data in an incompressible zero-pressure-gradient turbulent boundary layer over a flat plate. Data for one-point third-, fourth-, and fifth-order velocity moments were extracted for this purpose from the DNS dataset collected by the Fluid Dynamics Group at the Universidad Politécnica de Madrid at two streamwise locations Re_θ = 4101 and 5200. The comparison of DNS profiles for fifth-order velocity moments with those obtained using the truncated Gram-Charlier series expansions demonstrated that the truncated Gram-Charlier series expansions are an accurate approximation for all generated fifth-order velocity moments in the considered flow. Similar results were obtained using DNS data in a 2D fully developed channel flow (Jeyapaul et al., 2014).

Acknowledgments

A part of the presented material is based upon work supported by National Aeronautics and Space Administration under award NNX12AJ61A and by the Junior Faculty University of New Mexico - Los Alamos National Laboratory Collaborative Research Grant. B. E. Kaiser and S. V. Poroseva wish to thank the Center for Advance Research Computing at the University of New Mexico for providing the access to high-performance computing facilities and IT support.

References

Alfredsson, P. H., Johansson, A. V., Haritonidis, J. H., Eckelmann, H., 1988. The Fluctuating Wall-Shear Stress and the Velocity Field in the Viscous Sublayer. Phys. Fluids. 31(5), 1026-1033.

Alfredsson, P. H., Segalini, A., Örlü, R., 2011. A New Scaling for the Streamwise Turbulence Intensity in Wall-Bounded Turbulent Flows and What It Tells Us about the "Outer" Peak. Phys. Fluids, 23(4) 041702.

Antonia, R. A., Atkinson, J. D., 1973. High-Order Moments of Reynolds Shear Stress Fluctuations in a Turbulent Boundary Layer. J. Fluid Mech. 58(3), 581-593.

Bienaymé, J., 1853. Considérations à l'Appui de la Découverte de Laplace sur la Loi de Probabilité dans la Méthode des Moindres Carrés. Compte Rendu des Séances de l'Académie des Sciences Paris. 37, 309-324.

Borrell, G., Sillero, J. A., Jimenez, J., 2013. A Code for Direct Numerical Simulation of Turbulent Boundary Layers at High Reynolds Numbers in BG/P supercomputers. Computers & Fluids, 80, 37-43.

Bukreev, V. I., Zykov, V. V., Kostomakha, V. A., 1975. One-Dimensional Probability Distribution Laws of Velocity Fluctuations in Turbulent Flow in a Circular Tube (in Russian). Izvestiia Sibirskogo Otdeleniia Akademii Nauk SSSR, Seriia Tekhnicheskikh Nauk. 13(3), 3-9.

Chebyshev, P. L., 1867. Des Valeurs Moyennes. J. de Mathématiques Pures et Appliquées. 2 Série. 12, 177-184.

Chou, P. Y. , 1945. On the velocity correlations and the solutions of the equations of turbulent fluctuation. Q. J. Appl. Math., 3, 38-54.

Daly, B. J., Harlow, F. H., 1970. Transport Equations in Turbulence. Phys. Fluids. 13, 2634-2649.

DeGraaff, D. B., Eaton, J. K., 2000. Reynolds-Number Scaling of the Flat-Plate Turbulent Boundary Layer. J. Fluid Mech. 422(1), 319-346.

DeGraaff, D. B., Webster, D. R., Eaton, J. K. 1998. The Effect of Reynolds Number on Boundary Layer Turbulence. Exp. Therm. Fluid Sci., 18(4), 341-346.

Durst, F., Jovanović, J., Johansson, T. G., 1993. On the Statistical Properties of Truncated Gram–Charlier Series Expansions in Turbulent Wall-bounded Flows. Phys. Fluids A. 4(1)**,** 118-127.

Frenkiel, F. N., Klebanoff, P. S., 1973. Probability Distributions and Correlations in a Turbulent Boundary Layer. Phys. Fluids. 16(6), 725-737.

Hanjalić, K., Launder, B., 2011. Modelling Turbulence in Engineering and the Environment. Cambridge University Press, Cambridge, UK.

Honkan, A., Andreopoulos, Y., 1997. Vorticity, Strain-Rate and Dissipation Characteristics in the Near-Wall Region of Turbulent Boundary Layers. J. Fluid Mech. 350, 29-96.

Hutchins, N., Nickels, T. B., Marusic, I., Chong, M. S., 2009. Hot-Wire Spatial Resolution Issues in Wall-Bounded Turbulence. J. Fluid Mech. 635, 103-136.

Jeyapaul, E., Coleman, G. N., Rumsey, C. L., 2014. Assessment of Higher-order RANS Closures in Decelerated Planar Wall-bounded Turbulent Flow. AIAA2014-2088. Proc. the AIAA Aviation and Aeronautics Forum and Exposition, Atlanta, GA, June 16-20.

Johansson, T. G., Davidson, L., 2006. The 11th ERCOFTAC Workshop on Refined Turbulence Modelling. ERCOFTAC Bulletin, 69-2006. The Czestochowa University of Technology, Czestochowa, Poland.

Kampé de Fériet, J., 1966. The Gram-Charlier Approximation of the Normal Law and the Statistical Description of Homogeneous Turbulent Flow near Statistical Equilibrium. David Taylor Model Basin Report No. 2013, Naval Ship Research and Development Center, Washington D.C.

Klewicki, J., 1994. On the Interactions between Inner and Outer Region Motions in Turbulent Boundary Layers, Ph.D. Dissertation, Michigan State University, East Lansing, Michigan.

Ku, H., 1966. Notes on the Use of Propagation of Error Formulas. J. Research of National Bureau of Standards-C. Engineering and Instrumentation. 70C(4), 263-273.

Kurbatskii, A. F., Poroseva, S. V., 1997. A Model for Calculating the Three Components of the Excess for the Turbulent Field of Flow Velocity in a Round Pipe Rotating about Longitudinal Axis. High Temperature. **35**(3), 432-440.

Kurbatskii, A. F., Poroseva, S. V., 1999. Modelling turbulent diffusion in a rotating cylindrical pipe flow. Int. J. Heat and Fluid Flow. 20(3), 341-348.

Leschziner, M. A., 2006. Modelling turbulent separated flow in the context of aerodynamic applications. Fluid Dynamics Research, 38, 174-210.

Ligrani, P. M., Bradshaw, P., 1987. Spatial Resolution and Measurement of Turbulence in the Viscous Sublayer Using Subminiature Hot-Wire Probes. Exp. Fluids. 5, 407-417.

Millionshtchikov, M. D., 1941. On the theory of homogeneous isotropic turbulence. C. R. Acad. Sci. SSSR. 32, 615-619.

Moin, P., Mahesh, K., 1998. Direct Numerical Simulation: A Tool in Turbulence Research. Ann. Rev. Fluid Mech. **30**(1), 539-578.

Monin, A.S., Yaglom, A. M., 1979. Statistical Fluid Mechanics: Mechanics of Turbulence. Vol.1(The MIT Press, Cambridge, Massachusetts, and London, England, the Fourth printing, Chap. 4.

Murlis, J., Tasi, H. M., Bradshaw, P., 1982. The Structure of Turbulent Boundary Layers at low Reynolds Numbers. J. Fluid Mech. 122, 13-56.

Nagano, Y., Tagawa, M., 1988. Statistical characteristics of wall turbulence with a passive scalar. J. Fluid Mech.. 196, 157-185.

Nagano, Y., Tsuji, T., 1994. Recent Developments in Hot- and Cold-Wire Techniques for Measurements in Turbulent Shear Flows near Walls. Exp. Therm. Fluid Sci., 9(2), 94-110.

Nakagawa, H., Nezu, I., 1977. Prediction of the Contributions to the Reynolds Stress from Bursting Events in Open-Channel Flows. J. Fluid Mech. **80**(1), 99-128.

Ölçmen, M. S., Simpson, R. L., Goody, M. C., 1999. An Experimental Investigation of Two- and Three-Dimensional Turbulent Boundary Layers. VPI-AOE-262.

Österlund, J. M., 1999. Experimental Studies of Zero-Pressure-Gradient Turbulent Boundary Layer Flow. Ph.D Dissertation, Royal Institute of Technology, Department of Mechanics, Stockholm, Sweden.

Parneix, S., Laurence, D., Durbin, P. A., 1998. A procedure for using DNS databases. J. Fluids Eng., Trans. ASME, 20, 40-47.

Pilipchuk, M. I., 1986. A Study of Statistical Characteristics of the Longitudinal Velocity Component in a Turbulent Flow in a Rotating Pipe (in Russian). Ph. D. Thesis, Moscow Physico-Technical Institute, Moscow.

Poroseva, S. V., 1996. High-Order Turbulence Closure in a Fully-Developed Flow in a Cylindrical Pipe (in Russian). Ph. D. Thesis, Novosibirsk State University, Novosibirsk.

Rumsey, C. L., Gatski, T. B., Sellers III, W. L., Vatsa, V. N., Viken, S. A., 2004. Summary of the 2004 CFD Validation Workshop on Synthetic Jets and Turbulent Separation Control. AIAA-2004-2217. Proc. the 2nd AIAA Flow Control Conference.

Schlatter, P., Örlü, R., 2010. Assessment of Direct Numerical Simulation Data of Turbulent Boundary Layers. J. Fluid Mech., 659, 116-126.

Schwarz, W. R., 1992. Experiment and Modeling of a Three-Dimensional Turbulent Boundary Layer in a 30 Degree Bend. Ph.D. Dissertation, Department of Mechanical Engineering, Stanford University.

Schwarz, W. R., Bradshaw, P., 1994. Term-by-term tests of stress-transport turbulence models in a three-dimensional boundary layer. Phys. Fluids. 6(2), 986-998.

Sellke, T. M., Sellke, S. H., 1997. Chebyshev Inequalities for Unimodal Distributions. The American Statistician. 51(1), 34-40.

Sillero, J. A., Jiménez, J., Moser, R. D., 2013. One-Point Statistics for Turbulent Wall-Bounded Flows at Reynolds Numbers up to $\delta^+ = 2000$. Phys. Fluids. 25(10), 1-15.

Simens, M. P., Jiménez, J., Hoyas, S., Mizuno, Y., 2009. A High-Resolution Code for Turbulent Boundary Layers. J. Comp. Phys. 228(11), 4218-4231.

Smith, R. W., 1994. Effect of Reynolds Number on the Structure of Turbulent Boundary Layers, Ph.D. Dissertation, Princeton University, New Jersey.

Smits, A. J., Monty, J., Hultmark, M., Bailey, S. C. C., Hutchins, N., Marusic, I., 2011. Spatial Resolution Correction for Wall-Bounded Turbulence Measurements. J. Fluid Mech. 676(1), 41-53.

Thiele, F., Jakirlic, S., 2007. The 12th ERCOFTAC/IAHR/COST Workshop on Refined Turbulence Modelling. ERCOFTAC Bulletin, 75-2007. The Czestochowa University of Technology, Czestochowa, Poland.

Tsinober, A., 2001. An Informal Introduction to Turbulence. Kluwer Academic Publishers.

Tsuji, Y., Fransson, J. H. M., Alfredsson, P. H., Johansson, A.V., 2007. Pressure Statistics and Their Scaling in High-Reynolds-Number Turbulent Boundary Layers. J. Fluid Mech. 585, 1-40.

Uberoi, M. S., 1953. Quadruple Velocity Correlations and Pressure Fluctuations in Isotropic Turbulence. J. Aero. Sci. 20(3), 197-204.

Vassberg, J. C., Tinoco, E. N., Mani, M., Rider, B., Zickuhr, T., Levy, D. W., Brodersen, O. P., Eisfeld, B., Crippa, S., Wahls, R. A., Morrison, J. H., Mavriplis, D. J., Murayama, M., 2014. Summary of the Fourth AIAA Computational Fluid Dynamics Drag Prediction Workshop. J. Aircraft. 51,1070-1089.

Walpole, R. E., 1969. Introduction to Statistics, 4th printing. The Macmillian Company, New York/Collier-Macmillian Ltd., London.

Vysochanskij, D. F., Petunin, Y. I., 1980. Justification of the 3σ Rule for Unimodal Distributions. Theory of Probability and Mathematical Statistics. 21, 25-36 (In Russian).

Vysochanskij, D. F., Petunin, Y. I., 1983. A Remark on the Paper "Justification of the 3σ Rule for Unimodal Distributions". Theory of Probability and Mathematical Statistics. 27, 27-29 (In Russian).

Younis, B. A., Gatski, T. B., Speziale, C. G., 2000. Towards a Rational Model for the Triple Velocity Correlations of Turbulence. Proc. R. Soc. Lond. A. 456, 909-920.

Zaets, P. G., Onufriev, A. T., Pilipchuk, M. I., Safarov, R. A., 1984. Dvukhtochechnye Korrelaytsionnye Funktsii Chetvertogo Porydka dlya Prodol'noi Skorosti v Turbulentnom Techenii vo Vrashchayushcheisya Otnositel'no Osi Truby (Fourth-Order Two-Point Correlation Functions for the Longitudinal Velocity in a Turbulent Flow in an Axially Rotating Pipe). VINITI, Moscow, 3831-84 (in Russian).